Dalton Transactions

Cite this: *Dalton Trans.*, 2012, **41**, 10652

www.rsc.org/dalton

PAPER

Ratiometric fluorescence off-on-off sensor for Cu^{2+} in aqueous buffer by a lower rim triazole linked benzimidazole conjugate of calix[4]arene†

Rakesh Kumar Pathak,[a] Vijaya Kumar Hinge,[b] Prasenjit Mondal[a] and Chebrolu Pulla Rao*[a,b]

Received 22nd February 2012, Accepted 19th June 2012
DOI: 10.1039/c2dt30432e

A benzimidazole appended triazole linked 1,3-diconjugate of calix[4]arene (**L**) has been synthesized and characterized. The conjugate **L** has been found to recognize Cu^{2+} among the thirteen different metal ions studied by exhibiting ratiometric fluorescence changes through newly generated excimer band at ~380 nm. Fluorescence *off–on–off* behavior has been clearly demonstrated on the basis of the binding variability of Cu^{2+} to **L**. The binding has been elicited through the changes observed in the fluorescence, ESI MS and ^{1}H NMR titrations. All the other metal ions studied do not show any new band and further do not interfere with the recognition of Cu^{2+} by **L**, even when these are present in the same medium. The structural features of both the mono- and di-nuclear complexes were established by DFT computational calculations and found to display highly distorted geometry about the copper centers that deviate from both the tetrahedral and the square planar.

Introduction

Copper is the third most abundant transition metal of the human body[1] by being present as cofactor of many metalloenzymes and its importance may be attributed to its redox nature.[2] Excessive intake of Cu^{2+} is hazardous because of its ability to generate reactive oxygen species (ROS) that interfere with cellular metabolism.[3] However, its deficiency is also related to various hematological disturbances and some neurological diseases.[4] Hence, the sensitive and selective quantification of Cu^{2+} using organically derivatized synthetic receptors in the biological as well as in the environmental medium has always been a great challenge.[5] Among the fluorescence based receptors, the ratiometric ones exhibit higher sensitivity and better reliability than the simple intensity based ones owing to the robust nature of the former towards other internal and external factors.[6,7] A number of calix[4]arene based fluorescence sensors have been reported in the literature for Cu^{2+}, but ratiometric ones are rather scarce.[7–9] In this regard the benzimidazole appended triazole linked calix[4]arene conjugate (**L**) has been synthesized and found to be a selective and sensitive ratiometric fluorescence *off–on–off* sensor for Cu^{2+} in aqueous-buffer-medium.

[a]*Bio-inorganic Laboratory, Department of Chemistry, Indian Institute of Technology Bombay, Powai, Mumbai 400 076, India*
[b]*Department of Biosciences & Bioengineering, Indian Institute of Technology Bombay, Powai, Mumbai 400 076, India.*
E-mail: cprao@iitb.ac.in; Fax: +91 22 2572 3480;
Tel: +91 22 2576 7162

†Electronic supplementary information (ESI) available: Syntheses, characterization, absorption, fluorescence, mass spectra, NMR titrations and computational calculations data of all compounds have been given in supporting information. CCDC 869697. For ESI and crystallographic data in CIF or other electronic format see DOI: 10.1039/c2dt30432e

Results and discussion

The calix[4]arene conjugate **L** was synthesized by going through three reaction steps (Scheme 1), of which some precursors were already reported.[10,11] **L** has been characterized by various spectral techniques such as ^{1}H, ^{13}C NMR and high resolution ESI-MS (Experimental section and ESI, Fig. S1†) and its structure has been established by single crystal XRD (ESI, Table S1–S2†). The structure clearly shows that the arms are poised to form a 1 : 1 or 1 : 2 L : M^{n+} complex. Compound **3** was already reported by our group recently.[12]

Single crystal XRD structure of L

Single crystals of **L** suitable for X-ray diffraction study were obtained by slow diffusion of methanol into the solution of **L** in chloroform and the data were collected[13] (Experimental section). The calixarene unit adopts a cone conformation by forming intramolecular O–H···O hydrogen bonds (Fig. 1). In the lattice, one of the benzimidazole arms is bent and is stabilized through N–H···N hydrogen bonding with the other arm of the same molecule (Fig. 1). The hydrogen bonding data has been given in the ESI, Fig. S2 and Table S3†. Intermolecular π···π interaction was found between the bent benzimidazole rings emanating from the two neighboring molecules of **L** (Fig. 2).

Fluorescence titrations of L with metal ions

The receptor **L** exhibits fluorescence emission at ~310 nm when excited at 280 nm in methanol. Titration of this by Cu^{2+} results in a gradual quenching of the fluorescence emission at ~311 nm band and a new emission band appears at ~380 nm as a function

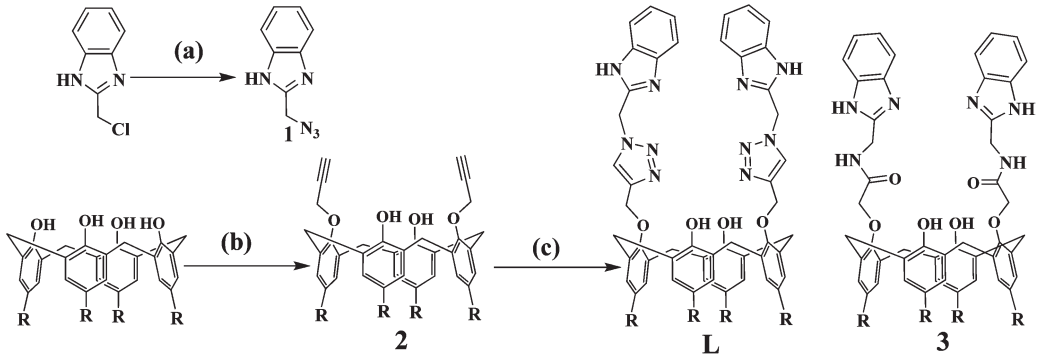

Scheme 1 Synthesis of benzimidazole appended triazole linked calix[4]arene conjugate, **L**: (a) NaN_3, DMF–EtOH (1 : 5), 5 h, reflux; (b) propargyl bromide, K_2CO_3, dry acetone, reflux, 24 h; (c) azidomethyl benzimidazole (**1**), $CuSO_4{\cdot}5H_2O$, sodium ascorbate, *t*-BuOH, dichloromethane and water, rt, 12 h. R = *tert*-butyl.

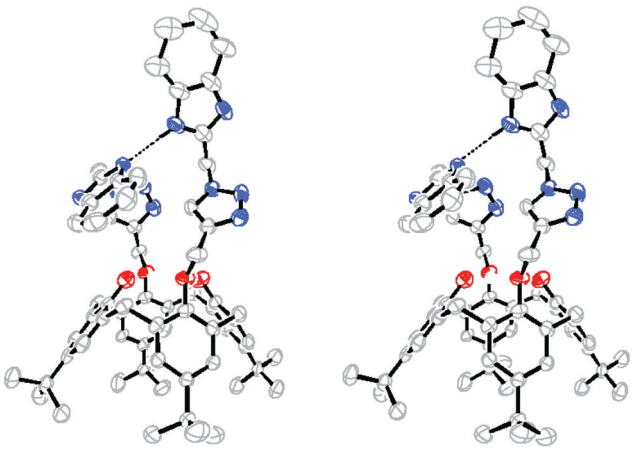

Fig. 1 ORTEP diagram for the stereo view of the molecular structure as obtained from the single crystal XRD of **L**.

of the increased Cu^{2+} concentration (Fig. 3a). The fluorescence intensity plots (Fig. 3b) shows gradual increase up to 2–3 equivalents and a decrease there after, upon addition of higher equivalents of Cu^{2+}.

In order to find the suitability of **L** to sense Cu^{2+} in aqueous buffer solution at physiological pH, fluorescence titrations were carried out in 50 mM aqueous HEPES buffer taken with methanol in a volume to volume ratio of 1 : 2 at pH = 7.4 to give an effective buffer concentration of 10 mM and this has been referred in this paper as "aqueous-buffer-medium". The fluorescence intensity is less in aqueous-buffer-medium as compared to pure methanol (Fig. 4 and 5). On going from methanol to the aqueous buffer, the fluorescence spectral behavior differs in the case of the 311 nm band, but remains same in the case of the 380 nm band (Fig. 4). All the other metal ions, *viz.*, Na^+, K^+, Mg^{2+}, Ca^{2+}, Mn^{2+}, Fe^{2+}, Co^{2+}, Ni^{2+}, Zn^{2+}, Cd^{2+}, Hg^{2+} and Pb^{2+}, used in the titrations do not show the development of a new band at ~380 nm, which was present only in the case of Cu^{2+} in both methanol as well as in aqueous-buffer-medium (Fig. 5). Similar fluorescence titrations of Cu^{2+} were also carried out with the control molecule (**3**) in order to elicit the role of triazole moiety present in **L**. The titration results suggest that the control molecule **3** does not show the new 380 nm band in presence of Cu^{2+} despite of having a similar quenching pattern (311 nm band) to that observed in the presence of **L** (ESI, Fig. S3†). The fluorescence titration carried out between **L** and Cu^{2+} by maintaining a 1 : 1 ratio clearly demonstrates that **L** can respond up to 9 ppb in methanol and 96 ppb in aqueous-buffer-medium (ESI, Fig. S4†). Thus, the fluorescence titrations clearly demonstrate that **L** can selectively detect and differentiate Cu^{2+} among the thirteen different metal ions studied (Fig. 5).

In order to ascertain that the new band observed at ~380 nm is from the excimer emission, the titration of **L** with Cu^{2+} has been performed in different solvents, *viz.*, methanol, ethanol, acetonitrile and THF, besides aqueous-buffer-medium (ESI, Fig. S5–S7†). Comparison of the results clearly supports the ~380 nm emission as emerging from the excimer. This is in line with the fact that the excimer formation is more favored in polar solvents as compared to the non polar ones. The excimer formation was further confirmed by carrying out the fluorescence titration experiments of **L** with Cu^{2+} in presence of ethidium bromide (EtBr). The excimer band was found to decrease in the presence of EtBr, which is expected to disrupt the excimer formed between the two benzimidazoles due to its intercalating nature (ESI, Fig. S8†). Therefore, it can be concluded that the emission band observed for **L** upon the addition of Cu^{2+} is mainly due to the excimer formation between the benzimidazole rings.

Absorption titration of L with Cu^{2+}

In order to obtain further support for Cu^{2+} binding, absorption titrations were carried out. The conjugate, **L** exhibited three absorption bands centered at ~274 and ~280 nm with a shoulder at ~293 nm. All these bands showed increase in the absorbance upon addition of Cu^{2+} and the absorbance was found to be saturated at ≥4 equivalents (Fig. 6). The isosbestic point observed at 285 nm indicates a transition between **L** and its copper bound species. A similar trend was observed when the absorption titrations of **L** were carried out with Cu^{2+} in aqueous-buffer-medium (ESI, Fig. S9†).

The stoichiometry of the complex was found to be 1 : 2 between **L** and Cu^{2+} based on the Job's plot[14] (ESI, Fig. S10†) and its association constant was found to be 7.24×10^9 and 1.80×10^{10} M^{-2} based on the fluorescence and absorption data, respectively.[15] A 1,3-diconjugate of calixarene similar to that of

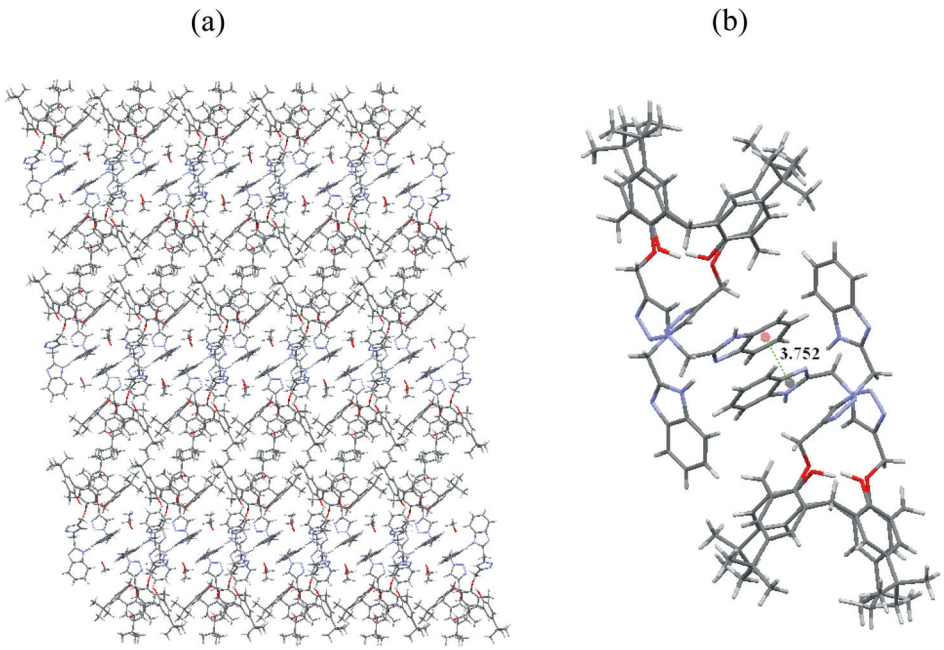

Fig. 2 (a) Crystal packing diagram of **L**; (b) diagram showing the intermolecular π···π interactions between two benzimidazole rings and the distance between them given in Å.

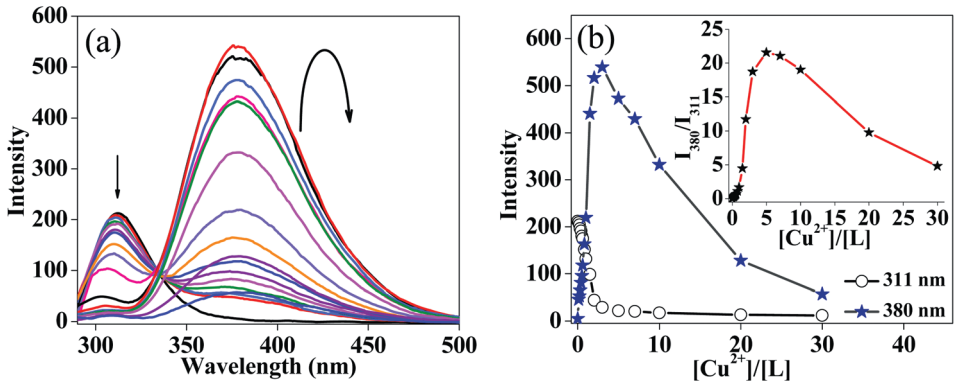

Fig. 3 Fluorescence titration of **L** with Cu^{2+} (λ_{ex} = 280 nm), [**L**] = 10 μM: (a) spectra obtained during the titration in methanol; (b) plot of fluorescence intensity as a function of [Cu^{2+}]/[**L**] mole ratio; inset shows ratiometric plot of I_{380}/I_{311} as a function of [Cu^{2+}]/[**L**] mole ratio.

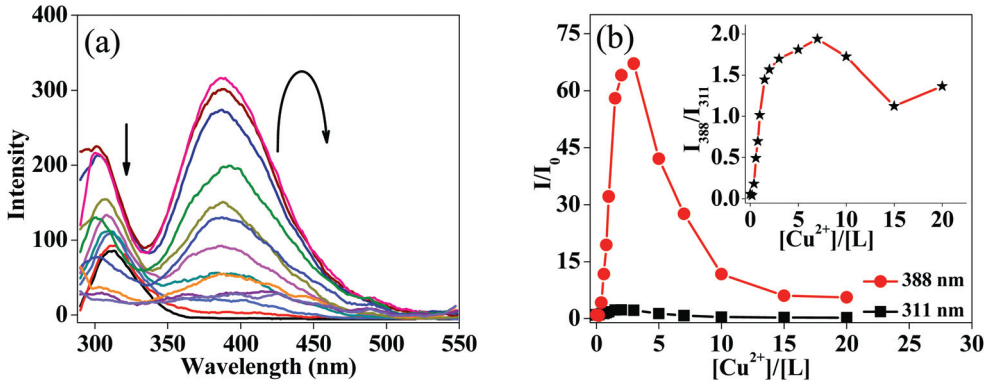

Fig. 4 Fluorescence titration of **L** with Cu^{2+} (λ_{ex} = 280 nm), [**L**] = 10 μM: (a) spectra obtained during the titration in aqueous-buffer-medium; (b) relative fluorescence intensity (I/I_0) as a function of [Cu^{2+}]/[**L**] mole ratio; inset shows ratiometric plot of I_{388}/I_{311} as a function of [Cu^{2+}]/[**L**] mole ratio.

L has been shown to have a comparable association constant.[8a] Absorption spectra recorded at higher concentrations of **L** and Cu^{2+} exhibited a d → d transition at 676 nm (Fig. 7). Thus, the absorption data supports that the **L** binds copper as Cu^{2+} and it remains as Cu^{2+} unlike that reported in the literature[8a,d] where calix[4]arene based conjugate reduces Cu^{2+} to Cu^{+}.

Competitive metal ion titrations

Competitive metal ion titrations were carried out to find whether **L** can selectively sense Cu^{2+} even in the presence of other metal ions. The results of the titrations showed that the fluorescence emission intensity of [**L** + Cu^{2+}] is unaltered in the presence of most of the metal ions except Hg^{2+} in methanol (Fig. 8). However, when the same titrations were carried out in aqueous-buffer-medium, the fluorescence of [**L** + Cu^{2+}] was unaltered in the presence of most of the metal ions including Hg^{2+}, hence the use of aqueous-buffer-medium is more advantageous over the use of simple methanol. Thus, in aqueous-buffer-medium, **L** is more selective compared to that in the pure methanol medium. Therefore, **L** can recognize Cu^{2+} even in the presence of other metal ions studied in aqueous-buffer-medium.

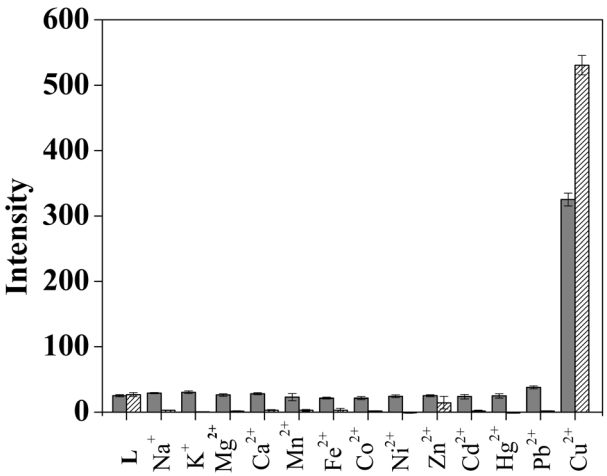

Fig. 5 Histogram showing the fluorescence response of **L** with different metal ions in MeOH (striped bars) and aqueous-buffer-medium (solid bars). [**L**] = 10 μM, [Cu^{2+}] = 30 μM.

EPR studies of the interaction of Cu^{2+} with L

In order to confirm that the bound copper is in (+2) rather than in (+1) state, unlike that reported in the literature for similar type of binding,[8a,d] EPR titrations were carried out. In one, the Cu(II) salt was titrated with varying amounts of calix[4]arene conjugate (**L**) and in the second it was the reverse. In the first set of titrations the signal corresponding to the simple Cu^{2+} transforms to a bonded species through exhibiting specific pattern (Fig. 9a). In the second set of titrations, the EPR signals of the bonded Cu^{2+} species starts to appear as the concentration of Cu^{2+} increases (Fig. 9b).

The pattern of EPR signals was found to be similar in both the types of titrations when the ligand to Cu^{2+} ratio was 1 : 2 (Fig. 9). Therefore, on the basis of EPR titrations it can be concluded that the Cu^{2+} is not being reduced to Cu^{+} while interacting with the calix[4]arene conjugate. This observation has been further strengthened by the absence of any ~438 nm band in absorption spectrum, which is otherwise found if the Cu^{2+} were reduced to Cu^{+} in the presence of phenolate moieties, as reported in the literature.[8a,d] Further, the presence of a d → d transition band observed at ~676 nm and the appearance of the green color supports the presence of Cu^{2+} bonded species, rather than Cu^{+} species (ESI, Fig. S11–S12†).

^{1}H NMR titration of L with Cu^{2+}

^{1}H NMR titrations were carried out to understand the mode of complexation of **L** with Cu^{2+}. Upon the initial addition of Cu^{2+} into the solution of **L** in DMSO-d_6, the proton NMR signals corresponding to the benzimidazole NH ('a'), triazole–H ('b'), benzimidazole–Ar–H ('d, e') and benzimidazole–CH_2 ('f') experiences considerable broadening owing to the binding of the paramagnetic Cu^{2+} in this region (ESI, Fig. S13†). However, the signals of the protons corresponding to the triazole–CH_2 ('g'), calixarene–CH_2 ('h') and the calixarene–OH ('c') experience changes only at higher concentrations of Cu^{2+}. On the basis of the ^{1}H NMR titrations it can be concluded that the Cu^{2+} initially binds to the benzimidazole region and upon addition of more equivalents, the additional Cu^{2+} goes to the phenolic lower rim region of the conjugate. Hence the possibility of binding two metal ions could be derived even based on the NMR titrations.

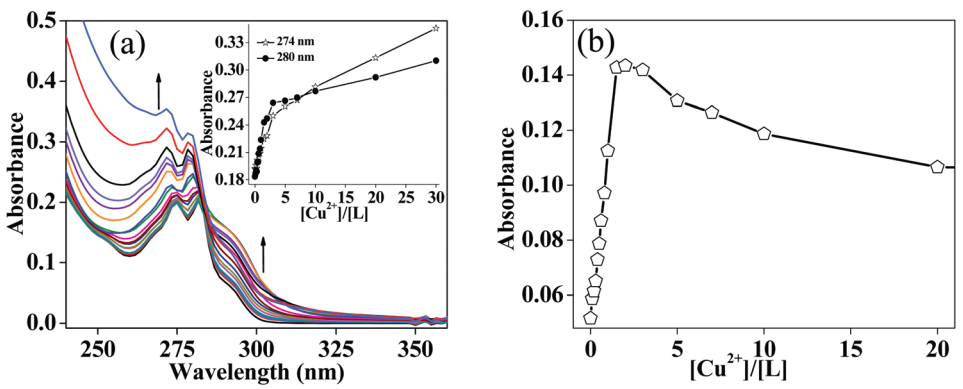

Fig. 6 (a) Absorption spectra obtained during the titration **L** with Cu^{2+} in methanol; inset shows the plot of absorbance *vs.* [Cu^{2+}]/[**L**] for 274 and 280 nm absorption bands. (b) Plot of absorbance *vs.* [Cu^{2+}]/[**L**] mole ratio for 293 nm band.

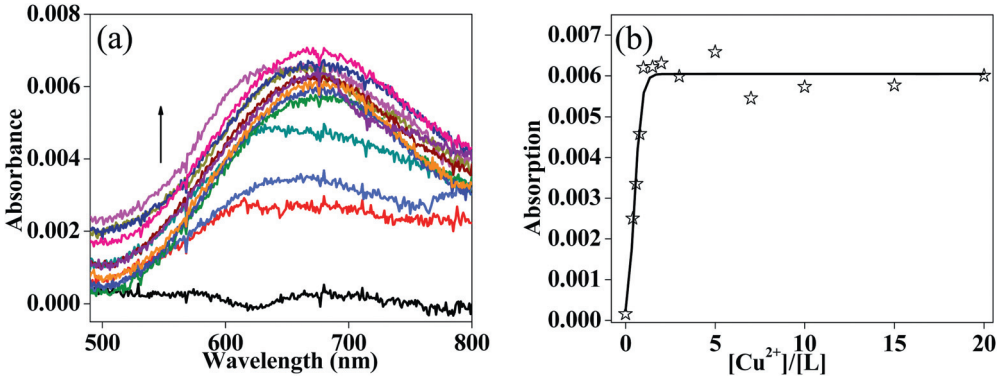

Fig. 7 Absorption titration of **L** with Cu^{2+}: (a) spectral traces in the region of 500–800 nm as measured at a higher concentration (100 μM) to show d → d transition in methanol. (b) Plot of absorbance *vs.* $[Cu^{2+}]/[\mathbf{L}]$ for d → d band observed at 676 nm.

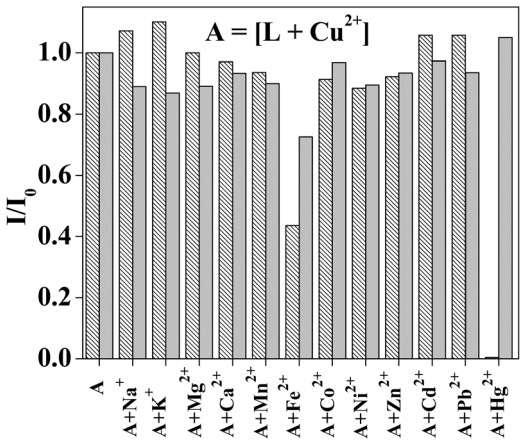

Fig. 8 Histogram showing the competitive metal ion titration response of $[\mathbf{L} + Cu^{2+}]$ with different metal ions (M^{n+}) in MeOH (striped bars) and aqueous-buffer-medium (solid bars). $[\mathbf{L}] = 10$ μM; $[Cu^{2+}] = 30$ μM; $[M^{n+}] = 30$ μM.

NMR titrations of **L** with Cu^{2+} have also been carried out in CD_3OD–$CDCl_3$ (6 : 1) mixture and found similar behavior (ESI, Fig. S13†) as that observed in DMSO-d_6.

Electrospray mass spectrometry

ESI-MS titrations of **L** with Cu^{2+} were carried out to find the stoichiometry of the complex formed (Fig. 10). Upon the titration of one equivalent of Cu^{2+} with **L**, a molecular ion peak at $m/z = 1133.52$ corresponding to a 1 : 1 ligand to metal ratio was observed. However, when the titration was carried out with more than two equivalents of Cu^{2+}, an additional molecular ion peak at ~1194.43 corresponding to 1 : 2 ligand to metal ratio was observed. The isotopic peak pattern observed for these molecular ion peaks resembles that of the calculated one, supporting the presence of metal ion and hence the complex formation (Fig. 10 and ESI, Fig. S14†).

Computational modeling of L with Cu^{2+}

L was found selectively to recognize Cu^{2+} (*switch-on*) through the formation of a 1 : 1 (**L**:M) complex initially followed by a 1 : 2 (**L**:M) complex at higher concentrations. Therefore, both the mononuclear, $[\mathbf{L}(Cu)]^{2+}$ and the dinuclear, $[\mathbf{L}(Cu)_2]^{2+}$ species of recognition were modelled by DFT calculations.[16] For computational ease, **L′** was used in place of **L** for optimizing its complexes (see the Experimental section). Thus, **L′**, $[\mathbf{L}'(Cu)]^{2+}$ and $[\mathbf{L}'_{-2H}(Cu)_2]^{2+}$ were optimized by DFT using Gaussian 03 package[16] as explained in the Experimental section and the corresponding optimized structures are shown in Fig. 11. The geometry optimization resulted in the conformational changes at the arms in order to accommodate two coppers. The conformational changes can be gauged through the dihedral angles of the arms (ESI, Table S4†) and the structure given in Fig. 11. In the process, the nitrogens of the triazole moieties turned to the interior of the calixarene to form a binding core. In the di-nuclear structure, the Cu1 exhibits an N_4 coordination by bonding through two benzimidazole and two triazole nitrogens, and the Cu2 exhibits an N_2O_2 coordination by bonding through two triazole nitrogens and two phenolate oxygens of the calix[4]-arene lower rim. Both the Cu^{2+} centers show highly distorted geometry that deviates from the square planar as well as from the tetrahedral (ESI, Table S5–S7†). A quantitative comparison of the metric parameters given in Fig. 11 leads to a conclusion that in the dinuclear complex while there is no specific preference for either of the geometries for the Cu1 center, Cu2 seems to fit better to a tetrahedral geometry than a square planar one. On the other hand, in case of the mononuclear structure, the copper is bound by the two benzimidazole and two triazole nitrogens to result in an N_4 binding core, but the distorted geometry fits better to a square planar than that of the tetrahedral, unlike that observed in case of the Cu1 in the di-nuclear complex.

Molecular orbitals (MOs) were calculated for **L′**, the mononuclear complex, $[\mathbf{L}'(Cu)]^{2+}$ and the dinuclear complex, $[\mathbf{L}'_{-2H}(Cu)_2]^{2+}$ using B3LYP/6-31G(d,p) level and the corresponding MOs are shown in (Fig. 12 and ESI, Fig. S15†). The percentages of the orbitals present on different fragments were calculated (ESI, Table S8†). In $[\mathbf{L}'(Cu)]^{2+}$ and $[\mathbf{L}'_{-2H}(Cu)_2]^{2+}$, HOMOs were found to be majorly localized on the arene core of calix[4]-arene, though these were extended onto the triazole and bezimidazole moieties. The LUMOs of $[\mathbf{L}'(Cu)]^{2+}$ are present more on the triazole as compared to the benzimidazole moieties. But in case of $[\mathbf{L}'_{-2H}(Cu)_2]^{2+}$ the LUMOs are majorly localized on both the binding cores. Therefore, the computational studies

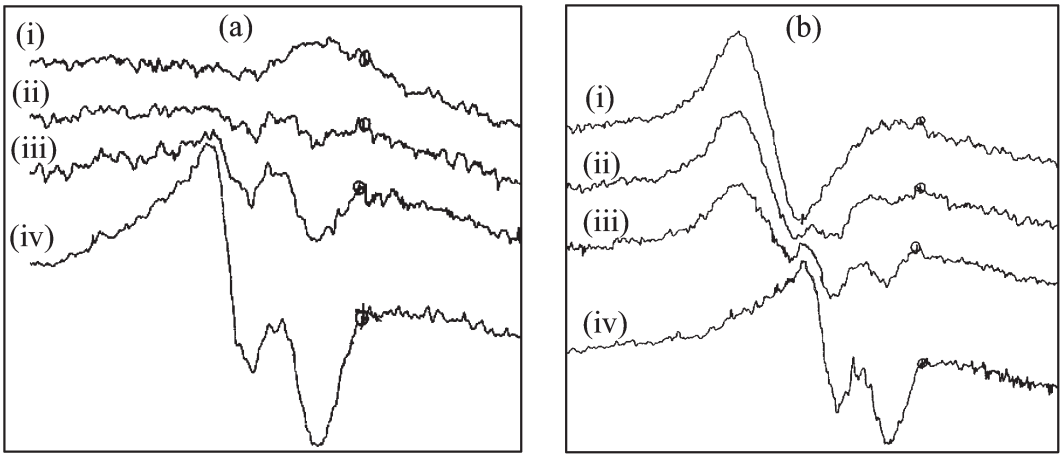

Fig. 9 EPR titrations for the interaction of **L** with Cu^{2+}: (a) spectral traces when **L** was titrated with varying amounts of Cu^{2+}, (i) 0, (ii) 0.25, (iii) 0.5, and (iv) 1.0 equiv. of Cu^{2+}; (b) spectral traces when Cu^{2+} was titrated with varying amount of **L**, (i) 0, (ii) 0.25, (iii) 0.5, and (iv) 1.0 equiv. of **L**.

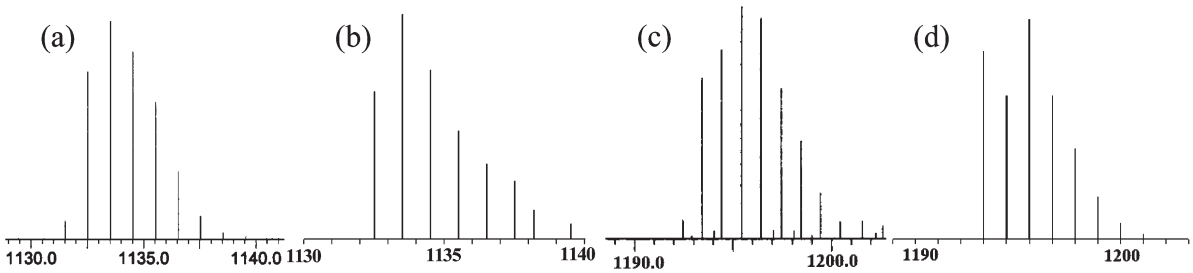

Fig. 10 ESI-MS spectra obtained in the titration of **L** with Cu^{2+}: (a) & (b) are for 1 : 1 (**L** : Cu^{2+}) complex, observed & calculated, respectively; (c) & (d) are for 1 : 2 (**L** : $2Cu^{2+}$) complex, observed & calculated, respectively.

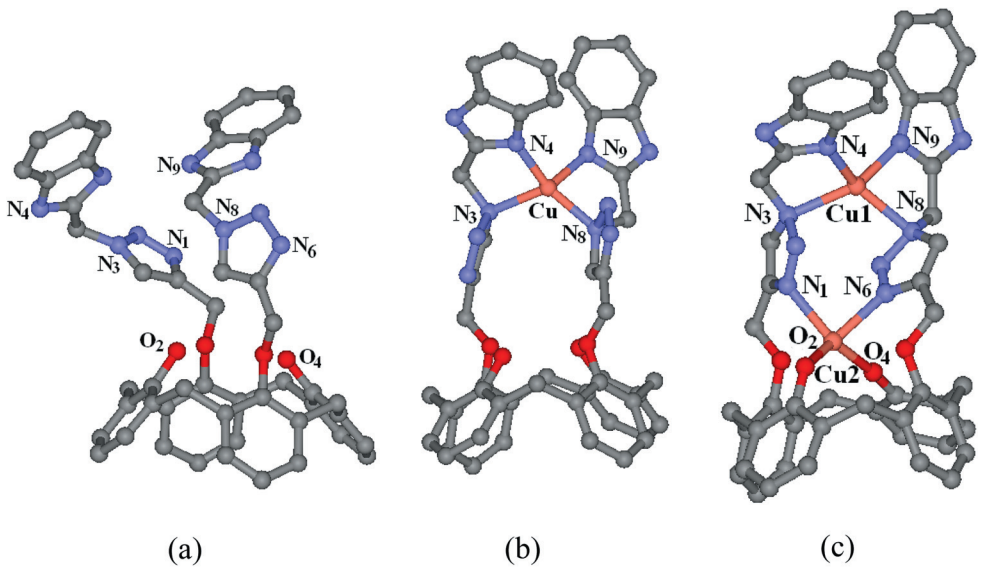

Fig. 11 B3LYP/6-31G(d,p) optimized structure of (a) **L′**, (b) mononuclear, $[\mathbf{L'}(Cu)]^{2+}$ and (c) dinuclear, $[\mathbf{L'}_{-2H}(Cu)_2]^{2+}$. Metric data [bond lengths (Å) and bond angles (°)]: Mono-nuclear complex, $[\mathbf{L'}(Cu)]^{2+}$: N_4–Cu = 1.991, N_9–Cu = 2.103, N_3–Cu = 2.177, N_8–Cu = 2.073 and N_4–Cu–N_9 = 100.0, N_4–Cu–N_3 = 84.7, N_4–Cu–N_8 = 151.4, N_9–Cu–N_3 = 126.8, N_9–Cu–N_8 = 83.1, N_3–Cu–N_8 = 116.2. Di-nuclear complex, $[\mathbf{L'}_{-2H}(Cu)_2]^{2+}$: Around Cu1: N_4–Cu1 = 2.120, N_9–Cu1 = 2.135, N_3–Cu1 = 2.243, N_8–Cu1 = 2.193 and N_4–Cu1–N_9 = 105.7, N_4–Cu1–N_3 = 80.4, N_4–Cu1–N_8 = 140.1, N_9–Cu1–N_3 = 145.3, N_9–Cu1–N_8 = 80.4, N_3–Cu1–N_8 = 116.8. Around Cu2: N_1–Cu2 = 2.191, N_6–Cu2 = 2.209, O_2–Cu2 = 1.944, O_4–Cu2 = 2.087 and N_1–Cu2–N_6 = 85.8, N_1–Cu2–O_2 = 96.5, N_1–Cu2–O_4 = 130.1, N_6–Cu2–O_2 = 138.1, N_6–Cu2–O_4 = 74.1, O_2–Cu2–O_4 = 128.6.

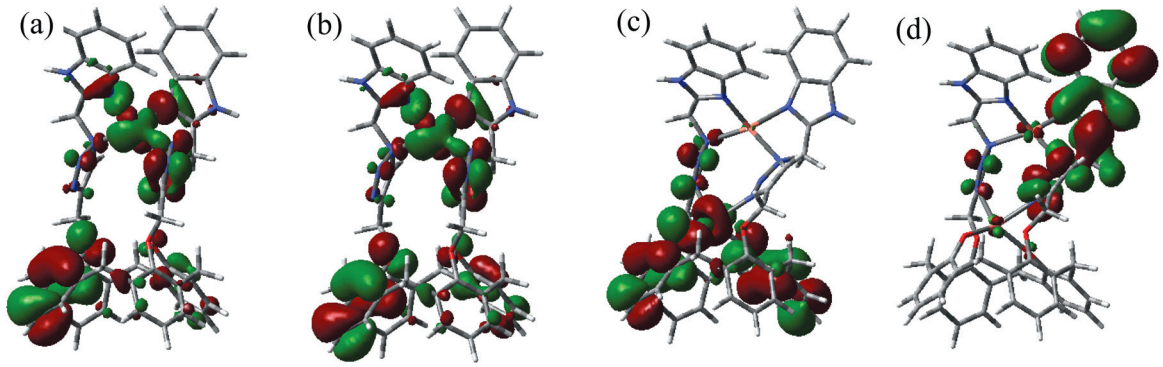

Fig. 12 Pictorial representation of the molecular orbitals (MOs) present on different fragments of (a) HOMO (β) of $[\mathbf{L}'(Cu)]^{2+}$, (b) LUMO (β) of $[\mathbf{L}'(Cu)]^{2+}$, (c) HOMO of $[\mathbf{L}'_{-2H}(Cu)_2]^{2+}$ and (d) LUMO of $[\mathbf{L}'_{-2H}(Cu)_2]^{2+}$.

further support the involvement of both the benzimidazole and triazole cores to bind Cu^{2+} in their mono as well as di-nuclear complexes.

Conclusions and correlations

The benzimidazole appended triazole linked calix[4]arene conjugate, **L** has been synthesized and characterized. The structure of **L** has been established based on single crystal XRD. The utility of **L** has been shown for the selective and sensitive recognition of Cu^{2+} among the thirteen different metal ions studied. The **L** shows ratiometric fluorescence changes with Cu^{2+} through exhibiting *off–on–off* fluorescence events. The new band appearing at ~380 nm in the fluorescence spectra is due to the excimer formation between the two benzimidazole moieties upon binding of **L** with Cu^{2+} in this region. The formation of excimer through the benzimidazole moieties has been further supported by fluorescence titrations carried out with EtBr as well as in different solvents. The excimer band initially increases up to the addition of 2–3 equivalents, while further addition (>3 equivalents) brings a decrease in the intensity (Fig. 13). Thus the fluorescence changes of **L** observed in the presence of Cu^{2+} are reminiscent of a traffic signal with three different color codes. This may be visualized as the band at ~310 nm due to the free **L** to a yellow signal, the new excimer band observed at ~380 nm upon the addition of Cu^{2+} up to ~3 equivalents to a green signal and the fluorescence quenching observed upon further addition of Cu^{2+} to a red signal.

The present studies including the mass spectra supports the formation of 1 : 1 complex initially, while the same is converted to 1 : 2 ($\mathbf{L} : Cu^{2+}$) at higher Cu^{2+} concentrations. The structural features of both the mono- and di-nuclear complexes were established by DFT based computational studies and found highly distorted geometries about the copper centers that deviate from both the tetrahedral as well as that of the square planar.

Experimental

Materials

All the metal perchlorate salts, *viz*., $NaClO_4 \cdot H_2O$, $KClO_4$, $Ca(ClO_4)_2 \cdot 4H_2O$, $Mg(ClO_4)_2 \cdot 6H_2O$, $Mn(ClO_4)_2 \cdot 6H_2O$, $Fe(ClO_4)_2 \cdot xH_2O$, $Co(ClO_4)_2 \cdot 6H_2O$, $Ni(ClO_4)_2 \cdot 6H_2O$, $Cu(ClO_4)_2 \cdot 6H_2O$, $Hg(ClO_4)_2 \cdot 4H_2O$, $Zn(ClO_4)_2 \cdot 6H_2O$, $Cd(ClO_4)_2 \cdot H_2O$ and $Pb(ClO_4)_2 \cdot H_2O$ were procured from commercial suppliers in India and the US. EPR measurements were made on a Varian model 109C E-line X-band spectrometer at room temperature and recorded at X-band with microwave power of 5 mW and microwave frequency of 9.1 GHz.

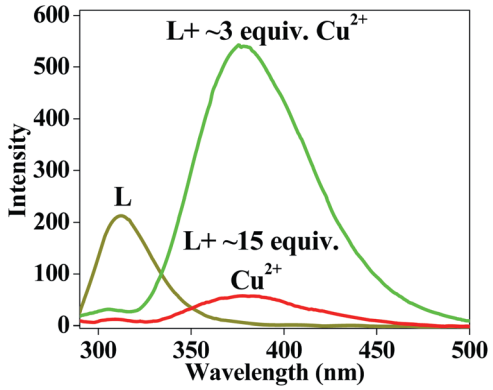

Fig. 13 Spectrum obtained for the fluorescence titration of **L** with various equivalents of Cu^{2+}.

Titrations

The bulk solutions of **L** and the metal perchlorate salts of Na^+, K^+, Mg^{2+}, Ca^{2+}, Mn^{2+}, Fe^{2+}, Co^{2+}, Ni^{2+}, Cu^{2+}, Zn^{2+}, Cd^{2+}, Pb^{2+}, and Hg^{2+} were prepared in MeOH, EtOH and aqueous-buffer-medium. Initially, a small amount (~3%) of $CHCl_3$ was used for dissolving the receptor **L**. All the measurements were made in a 1 cm quartz cell, and the effective concentration of **L** was maintained at 10 μM. In each case 50 μL of stock solution (6×10^{-4} M) of ligand was used, keeping the total volume fixed at 3000 μL. A 50 mM HEPES buffer stock solution was prepared with deionized water and 1000 μL (aqueous-buffer-medium) of this bulk solution is used for each titration of 3 mL solution. During the titration, the concentration of the metal perchlorate has been varied accordingly to result in requisite mole ratios of metal ion to **L**, and the total volume of the solution was maintained at 3 mL in each case by addition of aqueous methanol. A similar procedure was used to prepare the samples for UV-Vis studies. Several other solvent systems such as ethanol,

acetonitrile, THF and aqueous-buffer-medium have also been used to study the effect of Cu^{2+} on the fluorescence of **L**.

Computations

The computational calculations were carried out to find the mode of complexation of Cu^{2+} with **L**. As the formation of 1 : 1 (**L** : Cu) complex that is formed initially and then the formation of 1 : 2 [**L** : $(Cu)_2$] species has already been established by ESI-MS and were also supported by the other techniques, the species were optimized by computational calculations based on DFT using Gaussian 03 package.[16] The initial model for **L** was taken from the crystal structure reported in this paper. In order to reduce the computational times, before optimization **L′** was made simply by replacing the *tert*-butyl groups of **L** by hydrogens. The **L′** thus obtained was optimized by going through PM3 → HF/STO-3G → HF/3-21G → HF/6-31G → B3LYP/3-21G → B3LYP/6-31G in a cascade manner and both the complexes were optimized using B3LYP/6-31G(d,p). The output obtained at every stage was given as the input for the next higher level of calculations. In order to make the complex, $[\mathbf{L'}_{\mathbf{-2H}}(Cu)_2]^{2+}$, the phenolate OH groups were deprotonated and the resulting $(\mathbf{L'}_{\mathbf{-2H}})^{2-}$ was used for further studies. The complex formation was made initiated by placing the two Cu^{2+} far away from both the arms of $(\mathbf{L'}_{\mathbf{-2H}})^{2-}$ in such a way that the benzimidazole-N and triazole-N atoms are pointed towards the copper center. Similarly, the 1 : 1 complex, [**L′**(Cu)] was prepared and optimized. The molecular orbitals (MOs) were generated by using Gauss view software.[17]

Synthesis and characterization of 1[11]

To an aqueous solution (5 mL) of NaN_3 (0.780 g, 12.0 mmol) and DMF (2 mL), a solution of the chloromethyl benzimidazole (1.00 g, 6.00 mmol) in ethanol (10 mL) were added. After being heated under reflux for 5 h the solvent was evaporated to dryness. The residue was mixed with water and was extracted into chloroform. The combined extracts were dried over anhydrous Na_2SO_4 and the solvent was evaporated to dryness under vacuum. The precipitate was separated by filtration and washed with water. The crude product was recrystallized using chloroform–n-hexane mixture. ^{1}H NMR (400 MHz, DMSO-d_6) (ppm): 12.61 (s, 2H, benzimidazole-NH), 7.57–7.61 (two broad d, 2H, benzimidazole-Ar–H), 7.19 (s, 4H, benzimidazole-Ar–H), 4.61 (s, 4H, benzimidazole-CH_2), ^{13}C NMR ($CDCl_3$, 100 Hz) δ (ppm): 149.97, 149.77, 147.79, 147.63, 143.57, 142.32, 132.51, 129.97, 125.88, 125.42, 124.84, 123.17, 69.13, 48.24, 34.10, 34.01, 31.84, 31.11; HRMS *m*/*z* Calcd for $C_8H_7N_5$: 174.0780, Found 174.0777.

Synthesis and characterization of 2[10]

A mixture of potassium carbonate (5.10 g, 36.72 mmol) and *p-tert*-butylcalix[4]arene (10.0 g, 15.43 mmol) in dry acetone (200 mL) was stirred at room temperature for 1 h. To this, a, solution of propargyl bromide (6.49 g, 30.80 mmol) in dry acetone (50 mL) was added dropwise over a period of 30 min. The reaction mixture was refluxed for 24 h and was then allowed to cool to room temperature. The reaction mixture was filtered through celite to remove insoluble particles and the filtrate was concentrated by a rotatory evaporator. 100 mL of 2 M HCl was added to the concentrated reaction mixture and the product was extracted with dichloromethane (3 × 100 mL). The combined organic extracts were successively washed with water and brine (100 mL), dried over anhydrous Na_2SO_4, filtered and evaporated to dryness *in vacuo*. The crude product was recrystallized from CH_2Cl_2–CH_3OH to afford **2** as a white solid (9.10 g, 82% yield). ^{1}H NMR (400 MHz, $CDCl_3$) δ (ppm): 7.07 (s, 4H, Ar–H), 6.73 (s, 4H, Ar–H), 6.50 (s, 2H, OH), 4.74 (d, J = 2.4 Hz, 4H, OCH_2), 4.37 (d, J = 13.4 Hz, 4H, $ArCH_2Ar$), 3.33 (d, J = 13.4 Hz, 4H, $ArCH_2Ar$), 2.54 (t, J = 2.4 Hz, 2H, C≡CH), 1.30 (s, 18H, $(CH_3)_3$), 0.90 (s, 18H, $(CH_3)_3$). ^{13}C NMR ($CDCl_3$, 100 MHz) δ (ppm): 150.51, 149.62, 147.40, 141.77, 132.74, 128.16, 125.70, 125.19, 78.93, 63.45, 34.05, 34.02, 32.19, 31.88, 31.11; HRMS *m*/*z* Calcd for $C_{50}H_{60}O_4$: (M + H) 725.4570, Found 725.4576.

Synthesis and characterization of 3[12]

This compound was synthesized by adapting the procedure reported by us recently.[14] A suspension of 2-(aminomethyl)benzimidazole. 2HCl (2.73 g, 12.4 mmol) and Et_3N (6 mL, 43.1 mmol) were stirred in dry THF (100 mL) under argon atmosphere. The diacid chloride of calix[4]arene (4.32 g, 5.34 mmol) in dry THF (50 mL) was added dropwise to this reaction mixture. Immediately, a yellowish precipitate was formed and the stirring was continued for 48 h at room temperature. After filtration, the filtrate was concentrated to dryness. A yellow solid was obtained which was extracted with $CHCl_3$, washed with water and then with brine and the organic layer was dried over anhydrous Na_2SO_4. The filtrate was concentrated to dryness and recrystallized from EtOH–$CHCl_3$ to obtained **3** as white solid. Yield (55%, 2.95 g) ^{1}H NMR: ($CDCl_3$, δ ppm): 0.98 (s, 18H, $(C(CH_3)_3)$, 1.25 (s, 18H, $(C(CH_3)_3)$), 3.28 (d, 4H, Ar–CH_2–Ar, J = 13.30 Hz), 3.96 (d, 4H, Ar–CH_2–Ar, J = 13.30 Hz), 4.40 (s, 4H, –CH_2CONH–), 4.88 (d, 4H, –CONHCH_2–, J = 5.50Hz), 6.8 (s, 4H, Ar–H), 7.03 (s, 4H, Ar–H), 7.23–7.25 (m, 4H, benzimidazole), 7.53–7.55 (m, 4H, benzimidazole), 7.45 (s, 2H, –OH), 8.95 (t, 2H, –NH, J = 5.19). ^{13}C NMR: ($CDCl_3$, 100 MHz δ ppm): 31.10, 31.8, 32.1, 34.0, 34.2, 37.3, 73.8, 114.9, 124.1, 125.5, 126.1, 127.4, 135.5, 135.9, 142.7, 148.1, 149.2, 149.8, 152.0 and 170.6. HRMS *m*/*z* Calcd for $C_{64}H_{75}N_6O_6$: 1023.5784, Found 1023.5748.

Synthesis and characterization of L

Compound **2** (2.00 g, 2.76 mmol) was added to a solution of azidomethyl benzimidazole (1.43 g, 8.28 mmol) in 100 mL mixture of *t*-BuOH (25 ml), dichloromethane (25 ml) and water (50 ml). To this solution, $CuSO_4{\cdot}5H_2O$ (0.082 g, 0.33 mmol) and sodium ascorbate (0.218 g, 1.10 mmol) were added. The resulting solution was stirred for 12 h at room temperature. Upon completion of the reaction (checked based on TLC), the solvent was evaporated to dryness under vacuum. The crude product was dissolved in 50 mL dichloromethane and the organic layer was washed with water and brine (2 × 100 mL) followed by the treatment of organic layer with a saturated solution of EDTA to remove

excess Cu^{2+}. The separated organic layer was dried over anhydrous Na_2SO_4, and the solvent was removed *in vacuo*. The crude product was purified by column chromatography using petroleum ether and ethyl acetate followed by recrystallization from a chloroform–methanol mixture to give a solid product (2.16 g, 73% yield). ^{1}H NMR ($CDCl_3$, 400 MHz) δ (ppm): 8.05 (s, 2H, triazole-H), 7.50 (broad, 2H, benzimidazole-Ar–H, 7.35 (s, 2H, Ar–OH), 7.184–7.20 (m, 2H, benzimidazole-Ar–H), 7.01 (s, 4H, Ar–H), 6.79 (s, 4H, Ar–H), 5.92 (Ar–O–CH_2), 4.91 (s, 4H, AMBI-CH_2), 4.20 (d, 4H, Ar–CH_2–Ar), 3.25 (d, 4H, Ar–CH_2–Ar), 1.27 (s, 18H, Ar–C$(CH_3)_3$), 0.96 (s, 18H, Ar–C$(CH_3)_3$). ^{13}C NMR ($CDCl_3$, 100 MHz) δ (ppm): 149.97, 149.77, 147.79, 147.63, 143.57, 142.32, 132.51, 129.97, 125.88, 125.42, 124.84, 123.17, 69.13, 48.24, 34.10, 34.01, 31.84, 31.11; *m*/*z* (ES/MS) 1071.36 $[M]^+$ (100%); HRMS *m*/*z* Calcd for $C_{66}H_{74}N_{10}O_4$: 1071.5973, Found 1071.5945. Crystal parameters for **L**: empirical formula: $C_{137}H_{168}N_{20}O_{13}$; F. wt.: 2358.78; T (K) = 150(2); radiation: Mo Kα; wavelength/Å = 0.71073; crystal system: triclinic, $P\bar{1}$; unit cell dimensions: a = 11.7610 (3), b = 12.6977(4) and c = 25.9287(6) Å; α = 81.698(2), β = 83.283(2), γ = 64.155(3)°; V = 3441.96(16) Å^3; Z = 1; $D_{calc.}$ = 1.110 g cm^{-3}; μ = 0.072 (1/mm); F = 1232 (000); θ = 3.41, 25.0 (min, max); no. of unique reflections: 12 085; no. of parameters: 801; R_{obs}: 0.0743, w$R2_{obs}$: 0.2269; goof = 0.983.

Acknowledgements

CPR acknowledges the financial support from DST, CSIR and DAE-BRNS. RKP and VKH acknowledge CSIR for their fellowship. We thank Dr Venu Srinivas and Dr Shaikh M. Mobin for extending some help with the crystallography refinement.

References

1 B. G. Malmstrom and J. Leckner, *Curr. Opin. Chem. Biol.*, 1998, **2**, 286.
2 (*a*) L. Zeng, E. W. Miller, A. Pralle, E. Y. Isacoff and C. J. Chang, *J. Am. Chem. Soc.*, 2006, **128**, 10; (*b*) H. S. Jung, P. S. Kwon, J. W. Lee, J. I. Kim, C. S. Hong, J. W. Kim, S. Yan, J. Y. Lee, J. H. Lee, T. Joo and J. S. Kim, *J. Am. Chem. Soc.*, 2006, **128**, 10; (*c*) G. Peers and N. M. Price, *Nature*, 2006, **44**, 341.
3 (*a*) J. Diwedi and P. D. Sarkar, *J. Biochem. Tech.*, 2009, **1**, 104; (*b*) J. Y. Uriu-Adams and C. L. Keen, *Mol. Aspects Med.*, 2005, **26**, 268; (*c*) S. J. S. Flora, M. Mittal and A. Mehta, *Indian J. Med. Res.*, 2008, **128**, 501; (*d*) L. M. Gaetke and C. K. Chow, *Toxicology*, 2003, **189**, 147.
4 (*a*) V. Desai and S. G. Kaler, *Am. J. Clin. Nutr.*, 2008, **88**, 855S; (*b*) P. Zattaa and A. Frank, *Brain Res. Rev.*, 2007, **54**, 19; (*c*) T. R. Halfdanarson, N. Kumar, C.-Y. Li, R. L. Phyliky and W. J. Hogan, *Eur. J. Haematol.*, 2008, **80**, 523; (*d*) J. P. Fabisiak, V. A. Tyurin, Y. Y. Tyurina, G. G. Borisenko, A. Korotaeva, B. R. Pitt, J. S. Lazo and V. E. Kagan, *Arch. Biochem. Biophys.*, 1999, **373**, 171.
5 (*a*) D. T. Quang and J. S. Kim, *Chem. Rev.*, 2010, **110**, 6380; (*b*) D. W. Domaille, E. L. Que and C. J. Chang, *Nat. Chem. Biol.*, 2008, **4**, 168; (*c*) E. L. Que, D. W. Domaille and C. J. Chang, *Chem. Rev.*, 2008, **108**, 1517.
6 (*a*) B. Liu and H. Tian, *Chem. Commun.*, 2005, 3156; (*b*) J. F. Callan, A. P. de Silva and D. C. Magri, *Tetrahedron*, 2005, **61**, 8551; (*c*) S. H. Kim, J. S. Kim, S. M. Park and S.-K. Chang, *Org. Lett.*, 2006, **8**, 371; (*d*) X. Qi, E. J. Jun, L. Xu, S.-J. Kim, J. S. J. Hong, Y. J. Yoon and J. Yoon, *J. Org. Chem.*, 2006, **71**, 2881; (*e*) J. S. Kim and D. T. Quang, *Chem. Rev.*, 2007, **107**, 3780; (*f*) H. S. Jung, P. S. Kwon, J. W. Lee, J. I. Kim, C. S. Hong, J. W. Kim, S. Yan, J. Y. Lee, J. H. Lee, T. Joo and J. S. Kim, *J. Am. Chem. Soc.*, 2009, **131**, 2008.
7 (*a*) V. Dujols, F. Ford and A. W. Czarnik, *J. Am. Chem. Soc.*, 1997, **119**, 7386; (*b*) Q. Wu and E. V. Anslyn, *J. Am. Chem. Soc.*, 2004, **126**, 14682; (*c*) M. Dai, Z. Royzen and J. W. Canary, *J. Am. Chem. Soc.*, 2005, **127**, 1612; (*d*) Z. C. Wen, R. Yang, H. He and Y. B. Jiang, *Chem. Commun.*, 2006, 106; (*e*) K. M. K. Swamy, S.-K. Ko, S. Kwon, H. Lee, C. Mao, J.-M. Kim, K.-H. Lee, J. Kim, I. Shin and J. Yoon, *Chem. Commun.*, 2008, 5915; (*f*) H. J. Kim, J. Hong, A. Hong, S. Ham, J. H. Lee and J. S. Kim, *Org. Lett.*, 2008, **10**, 1963; (*g*) H. J. Kim, S. Y. Park, S. Yoon and J. S. Kim, *Tetrahedron*, 2008, **64**, 1294; (*h*) H. S. Jung, M. Park, D. Y. Han, E. Kim, C. Lee, S. Ham and J. S. Kim, *Org. Lett.*, 2009, **11**, 3378.
8 (*a*) I.-T. Ho, J.-H. Chu and W.-S. Chung, *Eur. J. Org. Chem.*, 2011, 1472–1481; (*b*) I. Leray and B. Valeur, *Eur. J. Inorg. Chem.*, 2009, 3525; (*c*) G.-Ke. Li, Z.-X. Xu, C.-F. Chen and Z.-T. Huang, *Chem. Commun.*, 2008, 1774; (*d*) A. Senthilvelan, I.-T. Ho, K.-C. Chang, G.-H. Lee, Y.-H. Liu and W.-S. Chung, *Chem.–Eur. J.*, 2009, **15**, 6152; (*e*) R. Joseph, J. P. Chinta and C. P. Rao, *Inorg. Chim. Acta*, 2010, **363**, 2833; (*f*) R. Joseph, B. Ramanujam, A. Acharya and C. P. Rao, *Tetrahedron Lett.*, 2009, **50**, 273; (*g*) M. Kumar, J. N. Babu and V. Bhalla, *J. Inclusion Phenom. Macrocyclic Chem.*, 2010, **66**, 139; (*h*) R. Kumar, V. Bhalla and M. Kumar, *Tetrahedron*, 2008, **64**, 8095; (*i*) O. Sahin and M. Yilmaz, *Tetrahedron*, 2011, **67**, 3501.
9 (*a*) J.-M. Liu, Q.-Y. Zheng, J.-L. Yang, C.-F. Chen and Z.-T. Huang, *Tetrahedron Lett.*, 2002, **43**, 9209; (*b*) Z. Liang, Z. Liu, L. Jiangc and Y. Gao, *Tetrahedron Lett.*, 2007, **48**, 1629; (*c*) Z. Xu, S. Kim, H. N. Kim, S. J. Han, C. Lee, J. S. Kim, X. Qian and J. Yoon, *Tetrahedron Lett.*, 2007, **48**, 9151; (*d*) K.-C. Chang, L.-Y. Luo, E. W.-G. Diau and W.-S. Chung, *Tetrahedron Lett.*, 2008, **49**, 5013; (*e*) H. J. Kim, S. H. Kim, J. H. Kim, L. N. Anh, a, J. H. Lee, C.-H. Lee and J. S. Kim, *Tetrahedron Lett.*, 2009, **50**, 2782; (*f*) D. T. Quang, H. S. Jung, J. H. Yoon, S. Y. Lee and J. S. Kim, *Bull. Korean Chem. Soc.*, 2007, **28**, 682; (*g*) R. Joseph, J. P. Chinta and C. P. Rao, *Inorg. Chem.*, 2011, **50**, 7050; (*h*) B. S. Creaven, D. F. Donlon and J. McGinley, *Coord. Chem. Rev.*, 2009, **253**, 893; (*i*) J. S. Kim and D. T. Quang, *Chem. Rev.*, 2007, **107**, 3780; (*j*) R. Joseph and C. P. Rao, *Chem. Rev.*, 2011, **111**, 4658.
10 (*a*) R. K. Pathak, A.G. Dikundwar, T. N. Guru Row and C. P. Rao, *Chem. Commun.*, 2010, **46**, 4345; (*b*) R. K. Pathak, S. M. Ibrahim and C. P. Rao, *Tetrahedron Lett.*, 2009, **50**, 2730; (*c*) S. Y. Park, J. H. Yoon, C. S. Hong, R. Souane, J. S. Kim, S. E. Matthews and J. Vicens, *J. Org. Chem.*, 2008, **73**, 8212.
11 K. Hidge and H. O. Hankovszy, *Synthesis*, 1978, **4**, 313.
12 R. Joseph, B. Ramanujam, A. Acharya, A. Khutia and C. P. Rao, *J. Org. Chem.*, 2008, **73**, 5745.
13 Crystal structure of L has been determined by single crystal X-ray diffraction. Single crystal XRD data were collected on an OXFORD DIFFRACTION XCALIBUR-S CCD system with graphite-monochromated Mo-Kα radiation by w – 2q scan mode and the absorption corrections were applied by using multi-scan method. The structural determinations by direct methods and the refinement of atomic parameters based on full-matrix least squares on F^2 were performed using the SHELX-97 programs (G. M. Sheldrick, *Acta Crystallogr., Sect. A*, 2008, **64**, 112). The 'PLATON 'SQUEEZE' command has been used to remove the disordered solvent contributions from the structure factor file.
14 (*a*) L. Praveen, V. B. Gnaga, R. Thirumalai, T. Sreeja, M. L. P. Reddy and R. L. Varma, *Inorg. Chem.*, 2007, **46**, 6277; (*b*) N. E. Polyakov, T. V. Leshina, E. O. Hand, A. Petrenko and L. D. Kispert, *J. Photochem. Photobiol., A*, 2004, **161**, 261.
15 M. I. Rodríguez-Càceres, R. A. Agbaria and I. M. Warner, *J. Fluoresc.*, 2005, **15**, 185–190.
16 M. J. Frisch, G. W. Trucks, H. B. Schlegel, G. E. Scuseria, M. A. Robb, J. R. Cheeseman, J. A. Montgomery, Jr., T. Vreven, K. N. Kudin, J. C. Burant, J. M. Millam, S. S. Iyengar, J. Tomasi, V. Barone, B. Mennucci, M. Cossi, G. Scalmani, N. Rega, G. A. Petersson, H. Nakatsuji, M. Hada, M. Ehara, K. Toyota, R. Fukuda, J. Hasegawa, M. Ishida, T. Nakajima, Y. Honda, O. Kitao, H. Nakai, M. Klene, X. Li, J. E. Knox, H. P. Hratchian, J. B. Cross, V. Bakken, C. Adamo, J. Jaramillo, R. Gomperts, R. E. Stratmann, O. Yazyev, A. J. Austin, R. Cammi, C. Pomelli, J. Ochterski, P. Y. Ayala, K. Morokuma, G. A. Voth, P. Salvador, J. J. Dannenberg, V. G. Zakrzewski, S. Dapprich, A. D. Daniels, M. C. Strain, O. Farkas, D. K. Malick, A. D. Rabuck, K. Raghavachari, J. B. Foresman, J. V. Ortiz, Q. Cui, A. G. Baboul, S. Clifford, J. Cioslowski, B. B. Stefanov, G. Liu, A. Liashenko, P. Piskorz, I. Komaromi, R. L. Martin, D. J. Fox, T. Keith, M. A. Al-Laham, C. Y. Peng, A. Nanayakkara, M. Challacombe, P. M. W. Gill, B. G. Johnson, W. Chen, M. W. Wong, C. Gonzalez and J. A. Pople, *GAUSSIAN 03 (Revision C.02)*, Gaussian, Inc., Wallingford, CT, 2004.
17 Pictures of the molecular orbital were generated by GaussView, Version 3.09, R. Dennington II, T. Keith, J. Millam, K. Eppinnett, W. L. Hovell and R. Gilliland, Semichem. Inc., Shawnee Mission, KS, 2003.

